

# Queen Alexandra Range 93069, 94269

Anorthositic regolith breccia

21.4, 3.1 g



Figure 1: QUE93069 as found in the Queen Alexandra Range of the Transantarctic Mountains, in 1993.

## Introduction

On the 1993 to 1994 ANSMET expedition, a small 21.4 lunar meteorite, Queen Alexandra Range (QUE) 93069 (Fig. 1), was discovered in the southern part of the Walcott Neve area, during foot search of a moraine deposit called Footrot Flats (Figs. 2 and 3). Although immediately recognized as a possible lunar meteorite, it was not until later more careful studies revealed it to be a feldpsathic or anorthositic regolith breccia. The next search season, 1994-1995, another paired 3.1 g piece of this breccia was discovered in the same morainal deposit – QUE 94269. At the time these were the 13<sup>th</sup> and 15<sup>th</sup> lunar meteorites known.

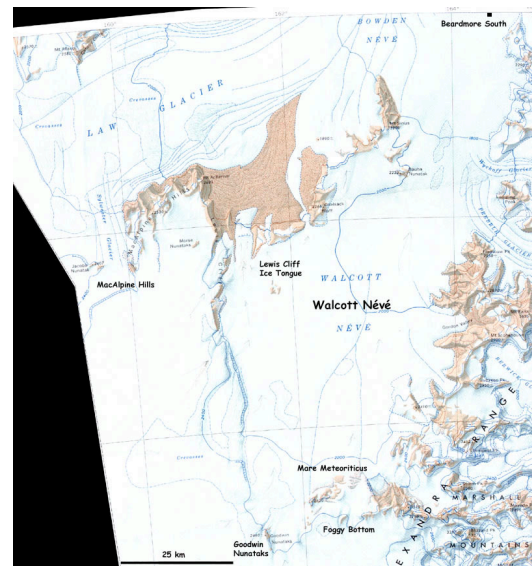
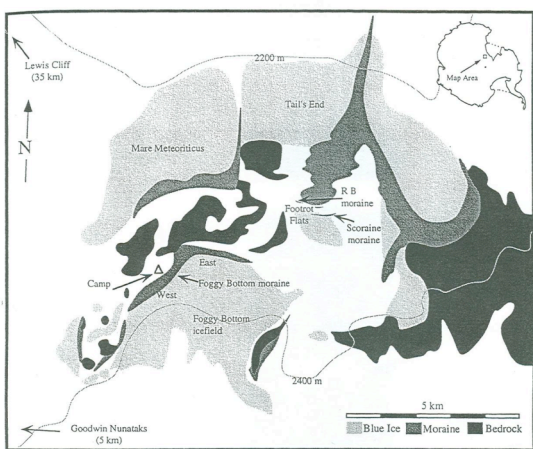


Figure 2: The Walcott Neve region of the Queen Alexandra Range, home of QUE meteorites. Foggy Bottom region is shown in the southern part of the map.



*Figure 3: Footrot Flats region where QUE 93069 and QUE 94269 were discovered.*

### **Petrography and Mineralogy**

QUE 93069 is a polymict feldspar-rich regolith breccia. This classification is based on the presence of abundant glass spheres, fine grained granulitic breccias, and with few to none preserving original igneous textures (Fig. 4 and Table 1). Also, metallic flakes are distributed throughout the matrix, and inhomogeneously between clasts (Lindstrom et al., 1995).

Mineral fragments include plagioclase feldspar ( $An_{96-98}$ ), olivine ( $Fa_{25-45}$ ), and two pyroxenes with unexsolved, finely exsolved, and coarsely exsolved occurrences, as well as clasts of orthopyroxene and pyroxferroite (Fig. 5; Korotev et al., 1996).

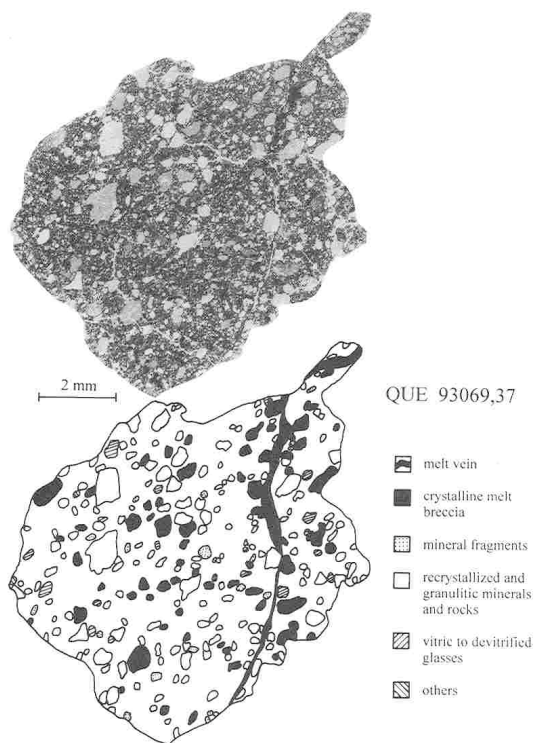


FIG. 1. Transmitted light photograph of the entire thin section of QUE 93069,37 and a sketch map showing the distribution of mineral and lithic clasts. An impact melt vein cuts across the entire thin section.

*Figure 4: Photomicrograph and sketch of section ,37 from the study of Bischoff (1996).*

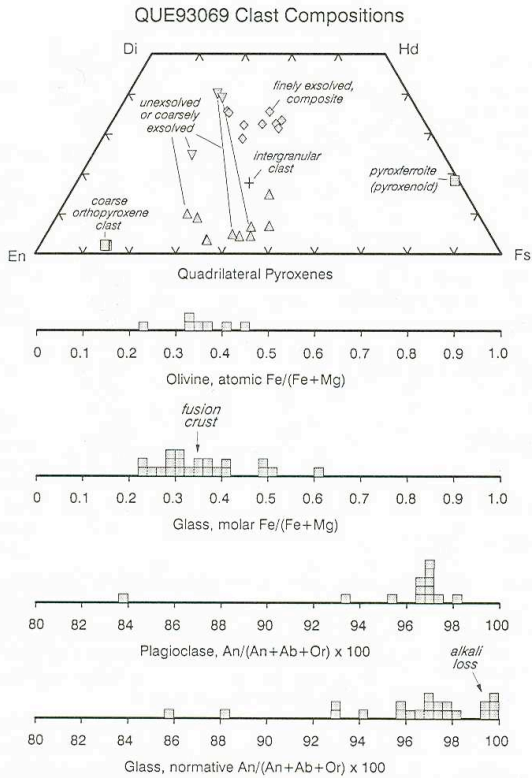


Figure 5: Clast compositions reported by Korotev et al. (1996) for QUE 93069.

## Chemistry

Many fractions of QUE 93069 have been analyzed by instrumental neutron activation analysis (INAA). Notable features of its bulk composition include its high  $\text{Al}_2\text{O}_3$ , Eu anomaly, and high concentrations of siderophile elements (Fig. 6 and 7). Also of significance is the absence of a KREEP component (e.g., Bischoff, 1998; Koeberl et al., 1996; Korotev et al., 1996). All of these characteristics indicate a high surface maturity level, in accord with the mineralogic and petrographic data.

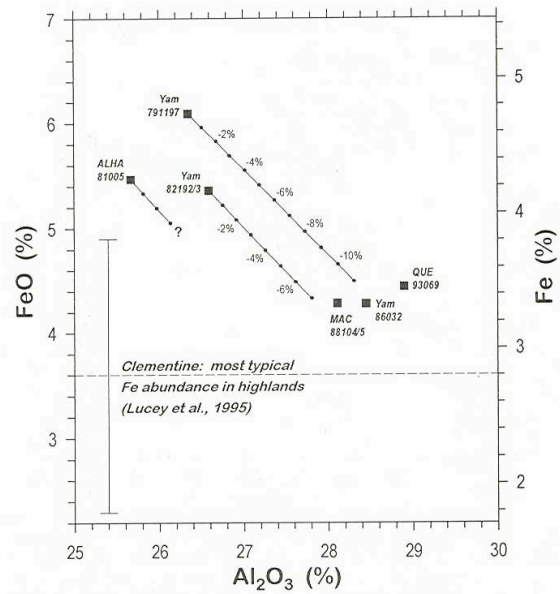


Figure 6:  $\text{FeO}$  vs.  $\text{Al}_2\text{O}_3$  for QUE 93069 as well as several other lunar meteorites (from Korotev et al. (1996).

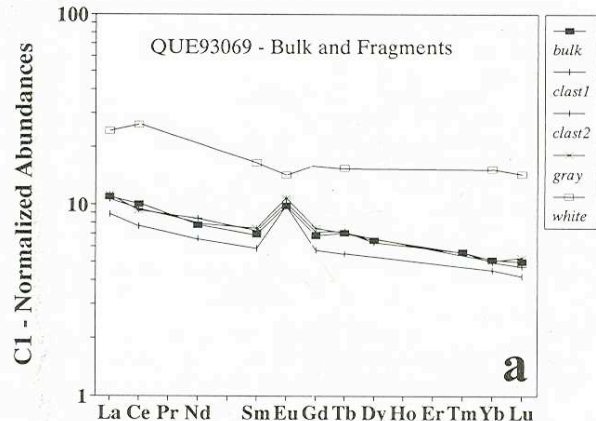


Figure 7: Rare earth element diagram for QUE 93069 bulk and fragments (from Koeberl et al., 1996).

Table 1: Modal analysis of QUE 93069, 37

Component	# clasts	Vol %
Granulitic anorthosite	20	4.9
Granulitic (gabbroic, noritic) anorthosite	17	5.5
Intergranularly recrystallized anorthosite	50	19.1
Recrystallized feldspathic melt breccianorite	33	15.0

<b>A) Recrystallized feldspathic rocks, breccias and granulitic lithologies</b>	<b>120</b>	<b>44.5</b>
Feldspathic fine-grained to microporphyritic crystalline melt breccia	54	21.9
Feldspathic subophitic crystalline melt breccia	13	5.2
Fine-grained mafic rich crystalline melt breccia	5	1.3
<b>B) Crystalline melt breccia</b>	<b>72</b>	<b>28.4</b>
Devitrified glass spherules	4	1.1
Impact glass fragments	10	2.4
Partly devitrified glass fragments	2	1.1
Impact melt with variolitic texture	1	0.3
Impact melt vein	1	10.1
<b>C) Devitrified impact glass</b>	<b>18</b>	<b>15.0</b>
Plagioclase mineral fragment	13	2.2
Intergranularly recrystallized plagioclase fragment	38	7.2
Mafic mineral fragment	10	2.6
<b>D) Mineral fragments</b>	<b>61</b>	<b>12.0</b>
<b>E) Cataclastic gabbro</b>	<b>2</b>	<b>0.2</b>
<b>Total</b>	<b>273</b>	<b>100.1</b>

(from Bischoff, 1996)

### Radiogenic age dating

There has been limited Rb-Sr, and Sm-Nd work on QUE 93069/94269.

$^{87}\text{Rb}/^{87}\text{Sr} = 0.013$  is a maximum for lunar meteorites. A best fit to lunar meteorite data (at the time), including Y86032, MAC 88105/4 and QUE 93069 indicates an age of  $4.74 \pm 0.049$  Ga (Fig. 8A), with a slope similar to the 4.56 Ga reference line for angrites. Results for the Sm-Nd system also indicate an old age for lunar meteorites – similar to a 4.56 Ga reference isochron (Fig. 8b).

Melt clasts from several lunar meteorites were sampled and analyzed by Cohen et al. (2000) for  $^{40}\text{Ar}/^{39}\text{Ar}$  analysis. They found a range of ages from 2.44 to 4.01 Ga, for five clasts and concluded that there may be two impact events recorded in QUE 93069 – one at 3.0 Ga and one at 3.87 Ga.

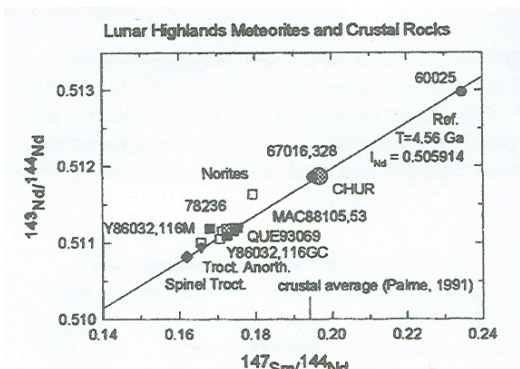
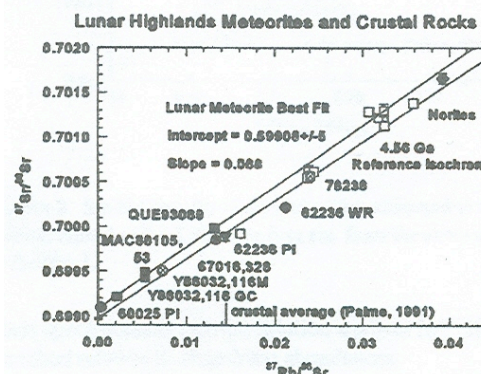


Figure 8: Rb-Sr and Sm-Nd isotopic data for QUE 93069 from the study of Nyquist et al. (1995).

### Cosmogenic isotopes and exposure ages

High concentrations of solar gases in QUE 93069 indicate that this meteorite resided in the lunar regolith and was exposed to the solar wind. The high concentrations have similarities to Luna 20 soil (Fig. 9). It contains very high concentrations of noble gases compared to other lunar meteorites (Thalmann et al., 1996; Swindle et al., 1995; Spettel et al., 1995). The  $^{40}\text{Ar}/^{36}\text{Ar}$  ratios indicate the meteorite was exposed to solar and lunar atmospheric volatiles ~400 Ma.

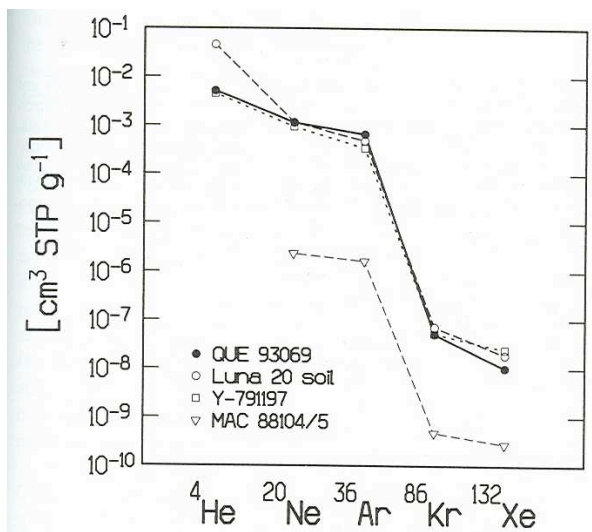


Figure 9: Trapped noble gasses in QUE 93069, reported by Thalmann et al. (1996).

FIG. 1 Elemental abundance pattern for the trapped noble gases in QUE 93069 lunar meteorite compared with that for lunar meteorites Yamato 791197, MAC 88104/5 and for Luna 20 highland soil.

**Table 2: Chemical composition of QUE 93069, QUE 94269**

	93069		93069						11a		11b		20a		20b		21a		21b	
	93069	fine	coarse	9a	9b	10a	10b	10c												
reference	1	2	2	3	3	3	3	3	3	3	3	3	3	3	3	3	3	3		
weight	58.38	?	?	24.4	27.7	23.3	20.3	21.9	22.3	30.5	31.3	19.3	32.3	27.9						
method	e	e	e	e	e	e	e	e	e	e	e	e	e	e	e	e	e	e		
SiO <sub>2</sub> %																				
TiO <sub>2</sub>																				
Al <sub>2</sub> O <sub>3</sub>																				
FeO	4.86	4.36	4.35	4.56	4.67	4.48	4.59	4.38	4.26	4.45	4.35	4.53	4.37	4.49						
MnO																				
MgO																				
CaO		16.4	16.3	16.2	16.2	16.4	16.2	16.4	16.1	16.4	16.3	16.1	16.1	16.4						
Na <sub>2</sub> O	0.40	0.354	0.350	0.352	0.353	0.356	0.355	0.356	0.351	0.353	0.354	0.357	0.355	0.361						
K <sub>2</sub> O	0.021																			
P <sub>2</sub> O <sub>5</sub>																				
S %																				
sum																				
Sc ppm	7.81	7.62	7.59	7.96	7.97	7.77	8.25	7.67	7.33	7.64	7.49	7.90	7.57	7.88						
V																				
Cr	626	599	603	645	652	599	597	574	568	607	595	606	571	617						
Co	25.1	23.7	22.9	22.5	23.0	22.8	20.7	18.5	22.5	23.4	21.5	21.6	22.3	22.2						
Ni	365	326	302	294	306	311	274	226	311	335	279	266	314	296						
Cu																				
Zn	15.8																			
Ga	4.6																			
Ge																				
As	0.11																			
Se	0.18																			
Rb	1.1																			
Sr	167																			
Y																				
Zr	72																			
Nb																				
Mo																				
Ru																				
Rh																				
Pd ppb																				
Ag ppb	30																			
Cd ppb																				
In ppb																				
Sn ppb																				
Sb ppb	42																			
Te ppb																				
Cs ppm	0.049						0.032	0.043	0.070	0.00	0.040	0.035	0.039	0.038	0.020	0.020	0.037	0.049		
Ba	51						39	46	48	40	33	40	40	43	47	37	44			

La	4.04	3.22	3.33	3.13	4.31	3.24	3.27	2.64	3.17	3.25	3.57	3.67	3.17	3.30
Ce	9.63			8.07	11.32	8.37	8.60	6.94	8.16	8.36	9.36	9.79	8.24	8.50
Pr														
Nd	5.55			4.9	6.9	4.6	5.0	4.3	5.1	5.3	5.5	4.9	5.5	5.5
Sm	1.61	1.52	1.54	1.519	2.120	1.556	1.599	1.266	1.525	1.558	1.743	1.771	1.538	1.582
Eu	0.86	0.83	0.82	0.832	0.835	0.841	0.819	0.814	0.818	0.828	0.834	0.847	0.822	0.835
Gd		2.1												
Tb	0.41			0.301	0.409	0.332	0.332	0.254	0.295	0.310	0.348	0.371	0.311	0.316
Dy		2.47												
Ho														
Er														
Tm	0.20													
Yb	1.27	1.23	1.26	1.167	1.385	1.188	1.248	0.995	1.143	1.187	1.290	1.326	1.163	1.214
Lu	0.19			0.162	0.188	0.169	0.178	0.142	0.160	0.164	0.179	0.187	0.162	0.171
Hf	1.24	1.13	1.32	1.15	1.19	1.15	1.28	0.93	1.12	1.16	1.25	1.37	1.13	1.17
Ta	0.18			0.146	0.151	0.144	0.139	0.112	0.151	0.155	0.158	0.195	0.143	0.149
W ppb	150													
Re ppb														
Os ppb														
Ir ppb	19.6	14.9	13.0	11.6	13.0	57.1	11.3	9.4	13.9	14.0	12.1	11.2	12.4	13.3
Pt ppb														
Au ppb	4.5	5.2	5.5	4.5	4.5	3.7	3.4	2.1	4.2	4.5	4.2	4.1	4.2	4.2
Th ppm	0.81			0.52	0.58	0.50	0.51	0.40	0.50	0.53	0.59	0.55	0.52	0.51
U ppm	0.19			0.15	0.13	0.14	0.16	0.11	0.13	0.16	0.12	0.15	0.11	0.16

technique (a) ICP-AES, (b) ICP-MS, (c) IDMS, (d) Ar, (e) INAA, (f) RNAA

references: 1 = Koeberl et al., 1996; 2 = Lindstrom, M. et al., 1995; 3 = Korotev et al., 1996

Lunar Meteorite Compendium by K Righter 2005

## Processing

QUE 93069 was processed in two stages with initial processing completed in April 1994, and the main stage of allocations in October 1994 (Fig. 10). QUE 94269 was processed in two stages with initial processing completed in May 1995, and the main stage of allocations in November 1995 (Fig. 11). Genealogy, sketches, and photographs showing where specific splits were taken are presented in Figures 12 to 14.

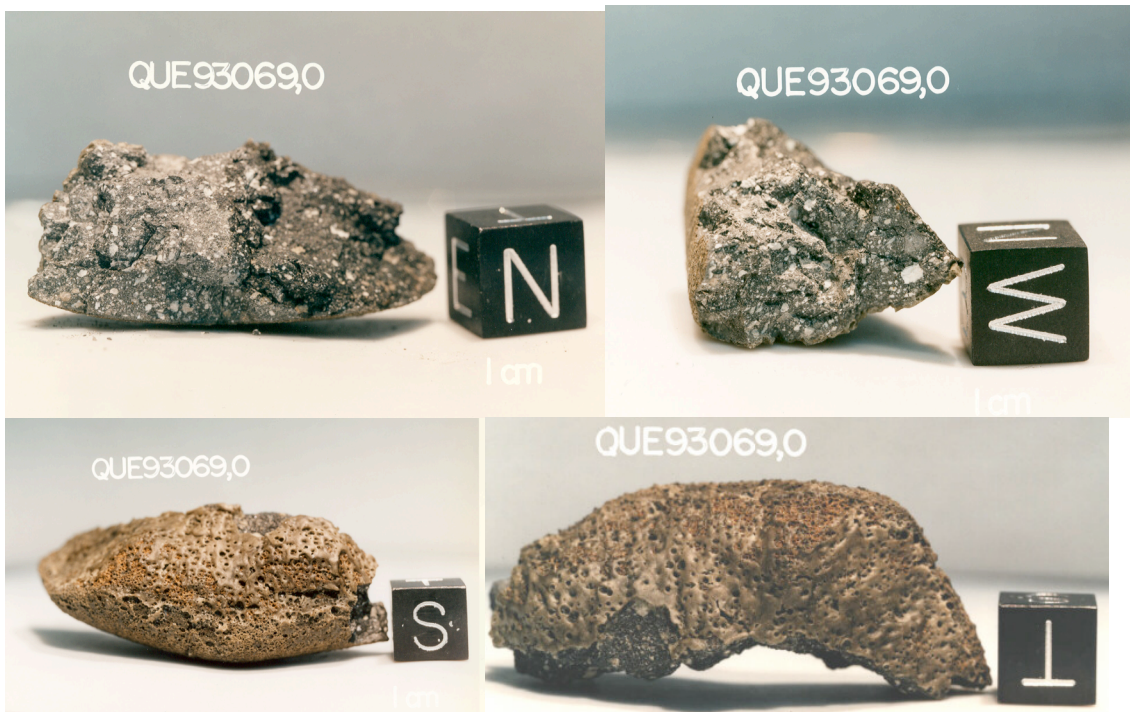
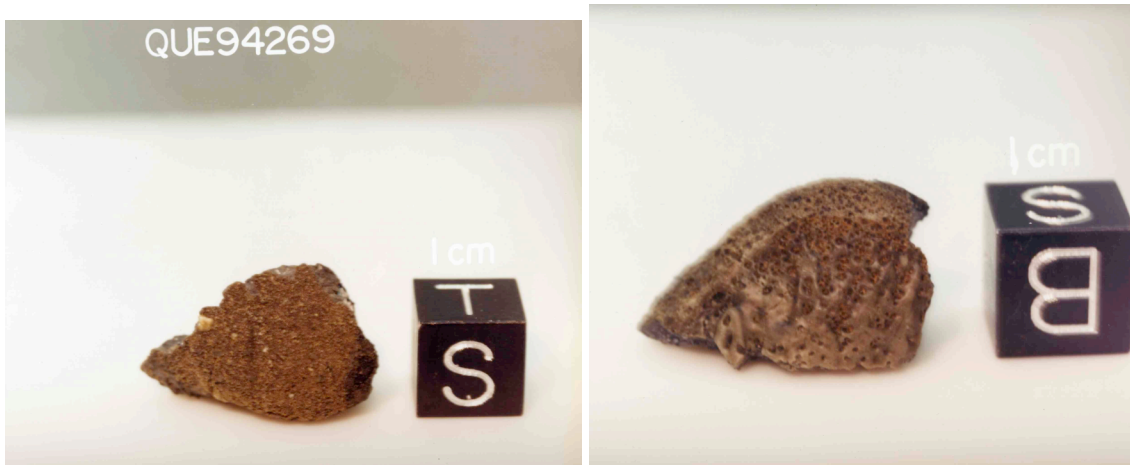


Figure 10: Four different views of QUE 93069 in the meteorite processing laboratory at JSC. Scale cube is 1 cm in all photos.



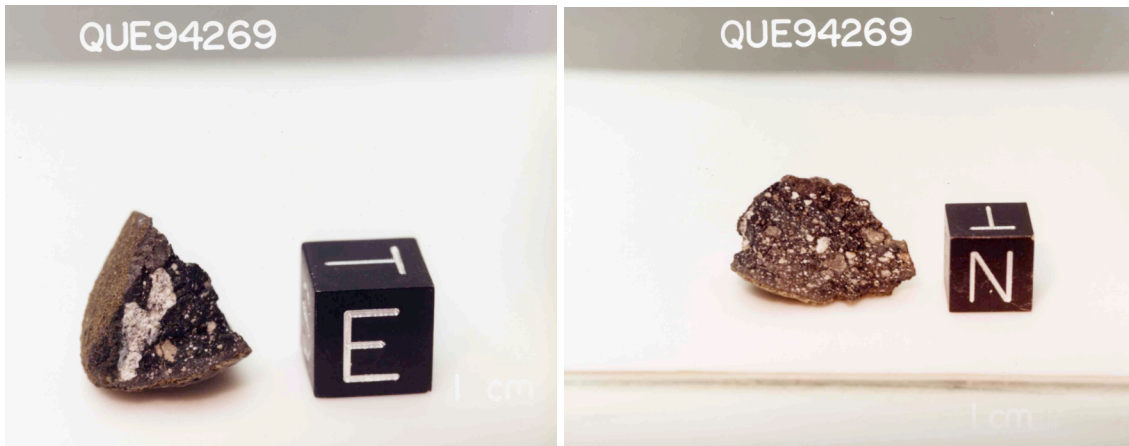


Figure 11: Four views of QUE 94269, paired with QUE 93069

**Table 3: Allocation history of QUE 93069**

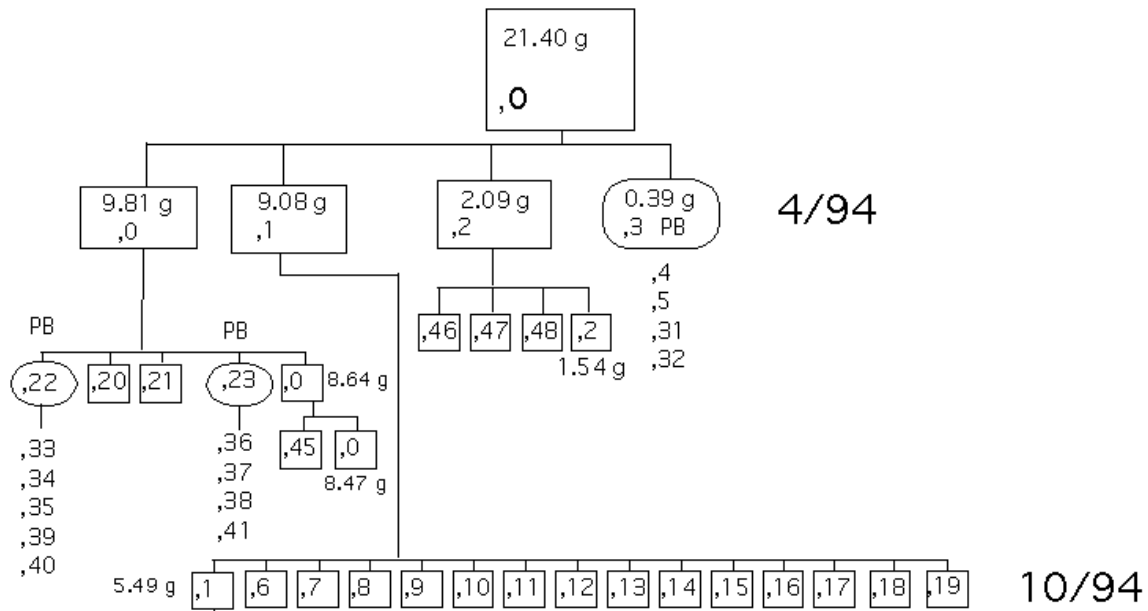
SPLIT	parent	TS	WEIGHT	LOCATION	DESCRIPTION
0			8.502	JSC	cps
1	0		4.665	JSC	cps + fines
2	0		1.58	JSC	cps + fines
3	0	entirely subdivided			potted butt
		4	0.01	JSC	thin section - silica
		5	0.01	SI	thin section - silica
		31	0.01	Haskin	thin section - silica
		32	0.01	JSC	thin section - silica
6	1		0.764	Dreibus	chips
7	1		0.037	Eugster	interior chips
8	1		0.608	Warren	interior chip
9	1		0.053	Haskin	interior chip
10	1		0.065	Haskin	interior chip
11	1		0.052	Haskin	interior chip
12	1		0.249	Kring	interior chip
13	1		0.158	Nishiizumi	interior chip
14	1		0.383	Nishiizumi	chip with fusion crust
15	1		0.053	Herzog	interior chip
16	1		0.215	Vogt	interior chip
17	1		0.305	Lindstrom M.	interior chip
18	1		0.107	Koeberl	interior chip
19	1		0.252	Nyquist	interior chip
20	0		0.051	Haskin	interior chip
21	0		0.061	Haskin	interior chip
22	0	entirely subdivided			potted butt
		33	0.01	JSC	thin section - silica

		34	0.01	JSC	thin section - silica
		35	0.01	Warren	thin section - silica
		39	0.01	Terada	thin section - silica
		40	0.01	JSC	thin section - silica
23	0	entirely subdivided			potted butt
		36	0.01	Treiman	thin section - silica
		37	0.01	JSC	thin section - silica
		38	0.01	Kring	thin section - silica
		41	0.01	Stoffler	thin section - silica
45	0	0.102		Jull	interior chips
46	2	0.12		Sears	interior chip
47	2	0.1		Vogt	interior chip
48	2	0.29		Zolensky	chip with fusion crust
49	1	0.668		JSC	potted butt
		52	0.01	JSC	thin section
		55	0.01	Noble	thin section
50	1	0.047		Franchi	interior chip
53	1	0.051		Noble	interior chip

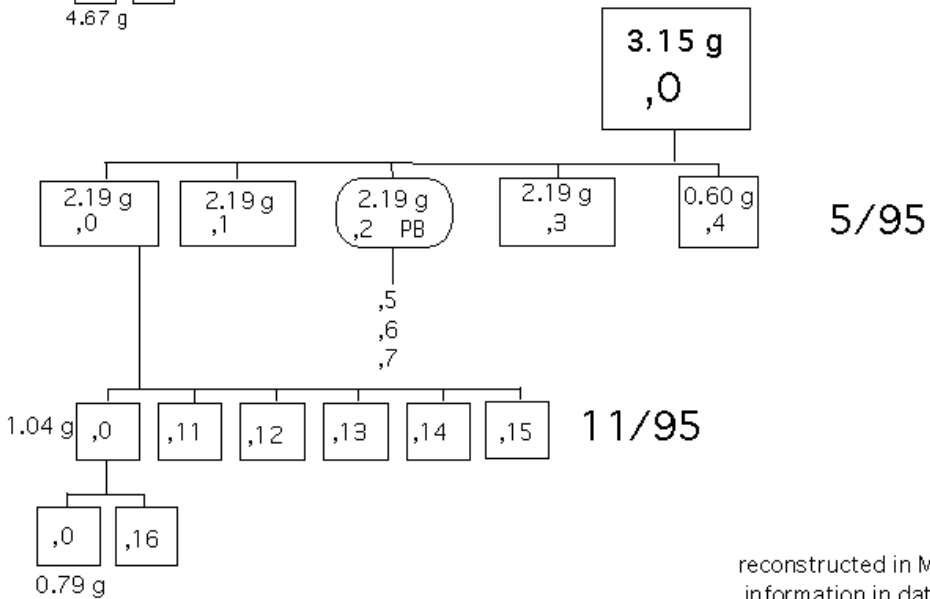
**Table 4: Allocation history of QUE 94269**

SPLIT	parent	TS	WEIGHT	LOCATION	DESCRIPTION
0			0.79	JSC	cps + fines
1	0		0.1	JSC	Clast A
2	0	entirely subdivided			potted butt
		5	0.01	SI	library thin section
		6	0.01	JSC	library thin section
3		entirely subdivided			potted butt
		7	0.01	McCoy	thin section
4	0		0.6	JSC	cps + fines
11	0		0.104	Lindstrom M.	interior chip
12	0		0.023	Eugster	interior chip
13	0		0.159	Nishiizumi	4 exterior chips / fusion crust
14	0		0.302	Warren	interior chips
15	0		0.562	JSC	exterior/interior chips
16	0		0.228	Korotev	interior chips

# QUE 93069



# QUE 94269



reconstructed in March 2005, from  
information in datapacks, by K. Righter

Figure 12: Genealogy of QUE 93069 and QUE 94269

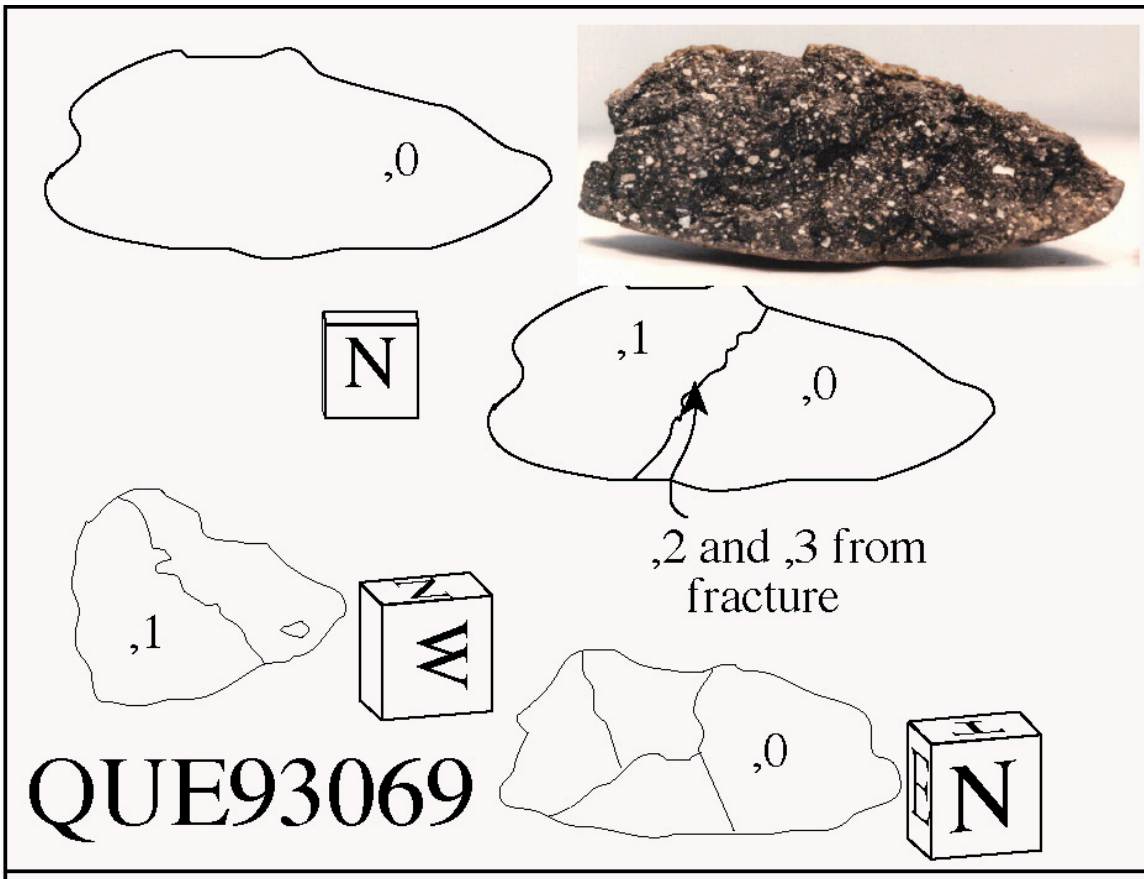


Figure 13: Summary of processing and allocation of QUE 93069, showing the masses from which many of the splits have been allocated.

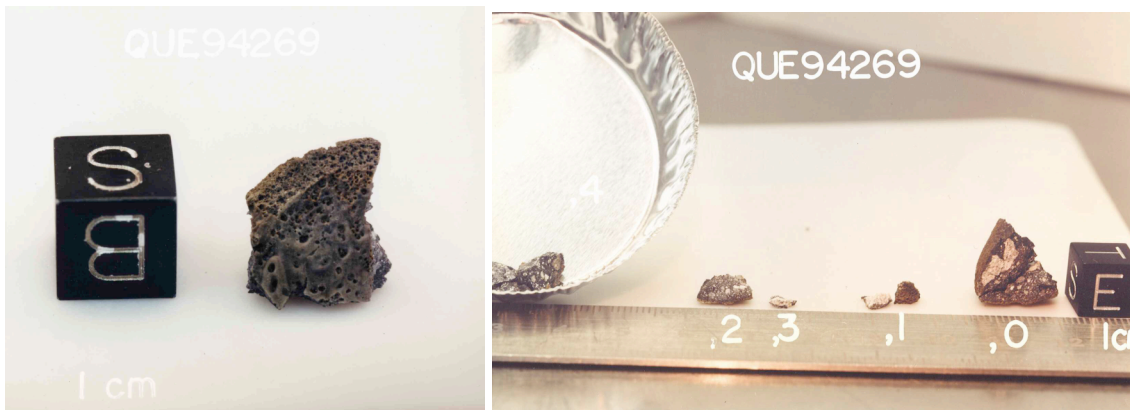


Figure 14: Post-processing chips of QUE 94269, showing the masses from which many of the splits have been allocated. On left is ,15 just before processing in Fall 1995. On right are splits 1, 2, 3 and 4 generated during initial processing.